

True Power Law Drilling Fluid Model: Effect of Its Rheological Parameters on Static Particle Settling Velocity

Mazen Ahmed Muherei¹, Saeed Salim Basaleh²

^{1&2} Assistant Professor, Department of Petroleum Engineering, Hadhramout University, Hadhramout, Yemen

Abstract - Adequate cuttings removal from the bottom hole of an oil well to the surface during a rotary drilling is critical for cost-effective drilling. The major factors that describe cuttings transport particularly in vertical sections are fluid effective viscosity and velocity which influence particle settling velocity. Rheological modelling of drilling fluids in oil fields is usually described by Bingham plastic and power law models. These models gain popularity because their specific descriptive parameters are fairly easy to estimate. Standard methods use Fann V-G Meter dial reading at 600 and 300 rpm to determine these rheological parameters. Unfortunately, these points correspond to higher shear rates which seldom prevail during particle settling. This work aims to investigate different shear rates to derive power law rheological parameters and show their influence on the magnitude of effective viscosity and hence settling velocity. The results show that data pair of R_{600}/R_3 was the best to predict the full spectrum of the fluid rheogram. Using Chien (1994) correlation, data pair of R_{200}/R_{100} give the best results for predicting observed settling velocity of a non-spherical particle settling in a static fluid. Data pair of R_{200}/R_{100} out performs commonly used data pairs (R_{600}/R_{300} , R_{100}/R_3 and R_6/R_3). Furthermore, Using modified Moore correlation with effective viscosity as suggested by Chien obtained excellent predictions with error less than 1% particularly with R_{600}/R_{100} .

Key Words: Drilling fluid, Drill cuttings, Hole cleaning, Rheological model, Settling velocity.

1. INTRODUCTION

Effective removal of cuttings is the primary task of any drilling fluid. Efficient hole cleaning is essential for the drilling practices to succeed and are required to complete the well at lower costs. Inadequate hole cleaning can trigger other wellbore problems which add to the well cost significantly. In vertical wells, cuttings tend to settle along the mud column and if this rate of settling is predicted accurately it is enough, for good hole cleaning, to pump the drilling fluid at a velocity greater than this settling velocity. However, drilling in deep water presents many

challenges and is characterized with narrow margins between formation pore pressure and fracture pressure gradients. Estimating cuttings settling velocity to be considerably higher or lower than actual will result in circulating the drilling fluid with either higher or lower velocities than required. Both of these are undesirable, since higher velocities will increase cost for unnecessary additional fluid, require higher pumping and fluid handling capacities, consume more power, increase erosion of uncased sections and increase frictional pressure loss [1].

The pressure loss may significantly increase up to the extent that violates allowable equivalent circulation density (ECD). As the drilling continues this way, the ECD becomes more critical and formation fracturing and lost of circulation (LOC) becomes the role than the exception. On the other hand, too low circulation velocities will cause less cuttings to be transported out of the well and more cuttings to accumulate in the annulus. Accumulated cuttings could significantly increase fluid column weight during circulation which may exceed the formation pore pressure that frequently develop to formation fracture and complete loss of the drilling fluid. Prediction of down word velocity of drill cuttings with a considerable degree of accuracy will assist in determining optimal circulation rate that will provide sufficient hole cleaning and yet minimizes fluid volume, power, and equipment requirements.

The ability of a drilling fluid to lift cuttings is affected by many factors and there is no universally accepted theory which can account for all the observed phenomena [2]. Several particle slip velocity correlations are available in the drilling literature, not the least are Chien [3], Zeidler [4], Moore [5], Walker and Mayes [6], Peden and Luo [7] and Chien [8]. These correlations have been developed in general from Newton's equation for predicting terminal velocities of spherical particles in Newtonian fluids. The principal differences are the way by which the non-Newtonian nature of the drilling fluids, the irregular shape of drill cuttings and the drag coefficient are taken into account in these correlations. Samble and Bourgoyne [9] have evaluated experimentally the correlations of Chien [3], Moore [5] and Walker & Mayes [6]. The experimental data used for this evaluation were obtained in Newtonian and non-Newtonian fluids for both static and flowing conditions. Among the evaluated correlations, the procedure proposed by Moore [5] gave the lowest average

error for all fluids studied. Furthermore, Skalle et al. [10] pointed that Chien [8] and Walker Mayes [6] correlations still have a good sound in petroleum industry. Furthermore, Chien [8] correlation was adopted by the API as the recommended procedure for drilling fluids [11].

Of most importance is the prediction of the drilling fluid's effective viscosity during the settling process. The apparent or effective viscosity represents the viscosity at the specific shear rate pertinent to that annular location in an annular flow situation, and does not necessarily represents the viscosity around the settling particles [7]. When fluid velocity approaches zero and the fluid becomes stagnant, effective viscosity will approach infinity.

Moore [5] suggested use of an effective viscosity term that is derived from equating pressure drop equation of Newtonian and power law fluids, while Chien [3] proposed use of an effective viscosity that is derived from equating pressure drop of Newtonian and Bingham plastic fluids. Accordingly, Moore [5] correlation employed the power law model parameters (K and n) that are basically determined at Fann viscometer readings of R_{600} and R_{300} to determine effective viscosity. Similarly Chien [3] correlation made use of Bingham plastic parameters (μ_p and YP) that are again determined from viscometer readings of R_{600} and R_{300} . However, API [12] methods for power law fluids recommend use of Fann viscometer readings of R_{100} and R_3 for calculating pressure loss inside the annulus. Becker and coworkers [13] stated that Fann rotary speed of 300 and 600 rpm induce shear rates higher than those that typically occur in actual drilling. Chien [8] emphasized that the effective viscosity working on the settling particles should be determined at the settling shear rate which is basically unknown. He recommended use of rheological parameters that are determined with a viscometer at low shear rates. However, Skalle et al. [10] stressed that the relative error is large at such low shear-stress readings.

There is thus a great distortion as which of the Fann viscometer readings should be used to determine the more representing rheological parameters. In this paper, the theory behind slip velocity correlations is presented. An example of drilling fluid was selected from literature. The Fann 35 VG meter 6 speed data were plotted and the fluid model identified. The rheological parameters are calculated using all shear stress/shear rate data pairs that can be obtained from a Fann 35 VG meter. The fluid rheogram was predicted again using previously calculated rheological parameters. Results were statistically compared. Finally the settling velocity according to Chien [3,8] are computed using different previously estimated rheological parameters. Settling velocity values are plotted and compared with regard to observed settling velocity.

2. THEORY OF SETTLING VELOCITY

2.1 Settling Velocity Concept

Settling velocity is commonly used as a measure of the ability of the drilling fluid to transport drill cutting in vertical wells. Traditionally, terminal velocity has been used in place of slip velocity; however, terminal and slip velocities are two different concepts. Terminal velocity is measured by dropping a single particle into a fluid; it does not account for particle interference or for accumulation of cuttings. It refers to the final constant falling velocity of a single particle in a calm fluid. Constant falling is achieved when buoyancy and resistance forces of the fluid balances the gravity of the particle. Terminal velocity is measured in a vertical direction, inaccuracy increases with increasing wellbore inclination [1].

Slip velocity refers to the velocity difference between the cuttings and the circulation fluid. Circulation fluid velocity varies across the flow area (depending on the flow regime). Fluid velocity near the wall is much smaller than the velocity near the centre of the flow area; cuttings and slip velocities varies accordingly across the flow area. However, slip velocity term is used to refer to the difference between the average fluid velocity and the average cuttings velocity rather than to the real slippage between cuttings and circulation fluid. Unlike terminal velocity which is always measured in the vertical direction, slip velocity is measured in the direction of flow.

2.2 Drag Coefficient Correlations

If one considers the forces acting on a discrete particle falling through a quiescent liquid, Newton's law for terminal velocity can be reached. Initially the particle will accelerate then at some point rather quickly the forces causing motion and those impeding motion will balance, thus the acceleration of the particle will become zero and will move with a constant velocity, called the terminal velocity. Ideally there are two forces acting on such a particle; the force developed as a result of friction between the particle and the liquid (F_D) and the force due to the effective weight of the particle which is the difference between gravity and buoyancy forces (F_g and F_B , respectively).

$$\begin{aligned}F_g &= Vg\rho_p \\F_B &= Vg\rho_l \\F_{eff} &= Vg(\rho_p - \rho_l)\end{aligned}\quad (1)$$

The frictional or drag force is less easy to quantify. Generally, it was found to be a function of the properties of both the liquid and the solid and can be expressed mathematically as:

$$F_D = C_D A_p \rho_l \frac{U_p^2}{2} \quad (2)$$

In accord to Newton's second Law, the forces should set equal to each other; that is:

$$Vg(\rho_p - \rho_l) = C_D A_p \rho_l \frac{U_p^2}{2} \quad (3)$$

By re-arranging of equation 3, for U_p gives:

$$U_p = \sqrt{\frac{2g}{C_D}} \sqrt{\frac{(\rho_p - \rho_l) V}{\rho_l A_p}} \quad (4)$$

For spherical particles V and A_p can be expressed in terms of particle diameter as:

$$V = \frac{\pi \times D_p^3}{6} \quad \& \quad A_p = \frac{\pi \times D_p^2}{4} \quad \text{then} \quad \frac{V}{A_p} = \frac{2}{3} D_p$$

Substituting the value of V/A_p in equation (4) gives:

$$U_p = \sqrt{\frac{4 \times g(\rho_p - \rho_l) D_p}{3 \times C_D \cdot \rho_l}} \quad (5)$$

Equation (5) is the Newton's law for terminal settling velocity of a spherical particle.

However, the drag coefficient in equation (5) has been found to be a function of the Reynolds Number:

$$C_D = \frac{24}{N_{RP}} + \frac{3}{N_{RP}^{0.5}} + 0.34$$

For very slow particle fall and laminar slip regime ($N_{RP} < 0.5$), Stokes reduced drag coefficient expression to [7]:

$$C_D = \frac{24}{N_{RP}}$$

Equation (5) becomes

$$U_p = \sqrt{\frac{4g(\rho_p - \rho_l) D_p^2 \rho_l U_p \times 100}{3 \times 24 \mu \rho_l}} \quad (6)$$

Squaring equation (6) and re-arranging for U_p again:

$$U_p = 100 \frac{g(\rho_p - \rho_l) D_p^2}{18\mu} \quad (7)$$

Equation (7) is the Stokes law for the terminal settling velocity of a spherical particle under laminar flow

conditions. In turbulent flow ($N_{RP} > 1000$) the drag coefficient becomes constant and Rittinger's equation ($C_D = 0.5$) may be used:

$$U_p = 51.15 \sqrt{\frac{(\rho_p - \rho_l) D_p}{\rho_l}} \quad (8)$$

2.3 Moore Settling Velocity Correlation

Moore [5] suggested use of an apparent Newtonian viscosity obtained by equating the laminar flow frictional pressure losses in the Newtonian model with frictional pressure losses in the power law fluid model; the following expression was resulted using c.g.s units:

$$\mu_a = \frac{K}{11.975} \left(\frac{(d_H - d_p)}{U_a} \right)^{(1-n)} \left(\frac{2 + \frac{1}{n}}{0.25} \right)^n \quad (9)$$

This correlation is for spherical particles and use average laminar flow velocity but does not account for the effect of particle slippage upon fluid shear stress. The friction factor (drag coefficient) in this correlation was obtained from slip-velocity experiments conducted with actual limestone and shale cuttings in mixtures of water and glycerine. Moore [5] pointed that for fully turbulent flow ($N_{RP} = 2000$), the friction factor remains constant at a value of about 1.5. Substituting this value in Newton's equation (eq. 5), the following relation was obtained:

$$U_p = 29.53 \sqrt{D_p \left(\frac{\rho_p - \rho_l}{\rho_l} \right)} \quad (10)$$

For laminar flow ($N_{RP} \leq 1$) the drag coefficient, according to Moore [5], was approximated to:

$$C_D = \frac{40}{N_{RP}}$$

Substitution in equation (5) gives:

$$U_p = 3270 \frac{D_p^2}{\mu_a} (\rho_p - \rho_l) \quad (11)$$

However, Moore [5] has pointed that equation (11) has a limited application since in most cases the particle Reynolds number will exceed 1.0 when the flow around the particle is laminar. Instead, Moore [5] has developed an equation for the drag coefficient that should be applied whenever the particle Reynolds number falls in the range of 10 to 100:

$$C_D = \frac{22}{\sqrt{N_{RP}}}$$

Similarly by substituting this value in equation (5), the following equation was attained:

$$U_p = 15.233 \frac{D_p}{\mu_a^{0.333}} \frac{(\rho_p - \rho_l)^{0.667}}{\rho_l^{0.333}} \tag{12}$$

2.4 Chien Settling Velocity Correlations

Chien [3,8] presented two empirical correlations for the settling velocity of drill cuttings for rotary drilling operations. Both for determination of the settling velocity of cuttings in all slip regimes. In 1972, Chien suggested use of a drag coefficient slightly different from that of equation (7); $CD = 24/N_{RP} + 1.714$. Substituting these values in equation 5, we approached at the following equation:

$$U_p = 0.07 \times \left(\frac{\mu_e}{\rho_l D_p} \right) \times \left[\sqrt{\frac{155741 \times D_p (\rho_p - \rho_l)}{\left(\frac{\mu_e}{\rho_l D_p} \right)^2 \left(\frac{\rho_p - \rho_l}{\rho_l} \right) + 1} - 1} \right] \tag{13}$$

However the equation published by Chien expressed in field units was [14]:

$$U_p = 0.0075 \times \left(\frac{\mu_e}{\rho_l D_p} \right) \times \left[\sqrt{\frac{36800 \times D_p (\rho_p - \rho_l)}{\left(\frac{\mu_e}{\rho_l D_p} \right)^2 \left(\frac{\rho_p - \rho_l}{\rho_l} \right) + 1} - 1} \right] \tag{14}$$

Where

V_s = Particle slip velocity, ft/sec

D_p = Particle diameter, in

ρ_p = Particle density, ppg

ρ_f = Fluid density, ppg

μ_e = Fluid effective viscosity, mPa.sec (cp)

Chien [8] emphasized on particle shape factor or sphericity (ψ). Particle sphericity is the ratio between the surface area of a sphere of volume equal to that of the particle and the surface area of the particle. Because a sphere has the minimum possible surface area of any shaped particle of the same volume, the value of sphericity is always less than or equal to 1. For a spherical particle, $\psi=1$; the greater the difference between the particle's shape and a spherical shape, the smaller the value of ψ .

Chien [8] stressed that majority of particles involved are irregularly shaped and the conveying fluid is commonly non-Newtonian in nature so neither Stoke's law nor Rittinger's equations are valid. Accordingly, he developed a correlation to predict settling velocity of irregularly shaped particles in Newtonian and non-Newtonian fluids for all types of slip regimes. In this correlation, the drag coefficient is approximated by: $CD = 30/N_{RP} + 67.289/e^{5.03\psi}$. Substituting this values in equation 5, we approached at the following equation:

$$U_p = 0.00223 \times e^{5.03\psi} X \times \left[\sqrt{\frac{3911734 \times e^{5.03\psi} D_p Y + 1}{X^2} - 1} \right] \tag{15}$$

Where $X = \frac{\mu_e}{\rho_l D_p}$ $Y = \frac{\rho_p - \rho_l}{\rho_l}$

The equation published by Chien [8] took the following form where viscosity is in Pa.sec and $\psi=0.7924$:

$$U_p = 120 \times \left(\frac{\mu_e}{\rho_l D_p} \right) \times \left[\sqrt{\frac{0.0727 \times D_p (\rho_p - \rho_l)}{\left(\frac{\mu_e}{\rho_l D_p} \right)^2 \left(\frac{\rho_p - \rho_l}{\rho_l} \right) + 1} - 1} \right] \tag{16}$$

Equation 16 has the same parameters as his previous equation (eq. 14) except for the numerical coefficients. Similarly, the equation adopted by API expressed in field units and took the following form:

$$U_p = 0.002403 \cdot e^{5.03\psi} X \left[\sqrt{\frac{920790 \cdot e^{5.03\psi} D_p Y + 1}{X^2} - 1} \right] \tag{17}$$

Where; $X = \frac{\mu_e}{\rho_l D_p}$ $Y = \frac{\rho_p - \rho_l}{\rho_l}$

2.5 Effective Viscosity

The settling problem of drilled cuttings in drilling fluids is complicated by the non-Newtonian behavior of these fluids, i.e. their shear-dependent viscosities. Theoretically the viscosity affecting the particle settling velocity in a non-Newtonian fluid should be that of the fluid envelop surrounding the particle and this viscosity depends on the shear rate distribution around the particle. Chien [3] suggested that, for water-based bentonite suspension, the

Bingham plastic viscosity could be used as an equivalent viscosity and for polymer type drilling fluids, the effective viscosity depends on annular fluid flow. Similarly, Moore [5] suggested an effective viscosity which depend on annular fluid flow. Accordingly, these viscosities are functions of the fluid velocity and are independent of the particle settling velocity. If the fluid velocity approaches zero, i.e. the fluid is stagnant, the effective viscosity for annular pipe flow will approach infinity and the settling velocity would be zero. According to Luo [15], this is obviously not true.

The effective viscosity suggested by Chien [8] is determined at the settling shear rate. The settling shear rate is the ratio of particle settling velocity to its particle diameter. The effective viscosity of power law fluid is equal to shear stress at that shear rate ($\mu_e = K\gamma^{n-1}$). Since the shear rate prevailing while the particle is settling out of the fluid is not known, a trial and error or numerical iteration method is required to predict the particle settling velocity in non-Newtonian fluid.

For non-Newtonian fluids, viscosity depends on the shear rate and knowledge of the settling shear rate is important for evaluating the viscous force experienced by the particle. In the turbulent regime the viscosity has a minor effect on drag force; therefore the settling shear rate has no important role in turbulent slip. However, for Newtonian fluids, viscosity is independent of the shear rate and the concept of a settling shear rate is not used. It should be pointed out that, in contrast to the previous suggestions, Chien [8] suggestion depends only upon the particle settling velocity and is independent of the fluid velocity. This is also a drawback that might affect settling velocity predictions.

3. RHEOLOGICAL MODEL

Rheology is classically defined as the study of the deformation and flow of matter. From a rheological perspective, drilling fluids are thixotropic (time-dependent) as well as temperature and pressure dependent. These fluids are visco-elastic exhibiting both viscous and elastic properties [16]. In conventional drilling, drilling fluids are modelled with classical rheological models like Bingham plastic or power law model and fluid behaviour is defined with only two points of the rheological relation (R_{600} and R_{300}). With increased use of polymer-based fluids as drilling fluids, the power law rheological model receives great attentions because it describes the behaviour of these fluids better than the Bingham plastic model [17]. The power law model can be expressed by:

$$\tau = K\gamma^n \tag{18}$$

The term "K" is defined as consistency index and describes the thickness of the drilling fluid. The exponent "n" is called flow behaviour index. There is no term for yield point and fluids that follow this model have no shear stress when shear rate is zero. The flow behavior index "n" indicate the degree of non-Newtonian. If values of "n" equal to unity the model reduces to Newtonian fluids. As the values of "n" become lesser than unity, the fluid shows shear-thinning properties and defined as pseudo-plastic fluid. At greater than unity n values the fluid shows shear-thickening properties and defined as dilatant. These rheological properties help evaluate consequences of fluid flow behaviour and critical decisions made continually based on these parameters [16].

3.1 Rheogram of Example Mud

The example drilling fluid was selected from Guliyev [18] study on settling velocity. The fluid composed 5% PHPA polymer-water mixture. The six Fann 35 VG meter dial readings and corresponding revolutions per minute as well as other fluid and particle properties are listed in table-1. The shear stress/shear rate data was plotted and fitted to a straight line (Bingham plastic model) and exponent line equations (power law model). As shown in Figure-1, the example mud follows power law model.

Table-1: Fluid and particle properties

RPM	600	300	200	100	6	3
Shear Rate, sec ⁻¹	1022	511	341	170	10	5
Dial Reading	63	46.5	39	29	8	6
Shear Stress, lb/100ft ²	67.2	49.6	41.6	30.9	8.5	6.4
Shear Stress, Pa	32.19	23.76	19.93	14.82	4.09	3.07
Fluid Density, g/cm ³	1.001		Particle density, g/cm ³		2.672	
Particle Size, cm	0.3387		Particle Sphericity		0.91	
Particle Settling Velocity in the Stagnant Fluid, cm/sec						0.7

3.2 Calculation of Rheological Parameters

To calculate "n" and "K" values, a mud's Fann 35 VG meter dial readings and corresponding revolutions per minute are required. Two data pairs are required for a solution. Generally, R_{600}/R_{300} are in common use. Chien [8] suggested use of R_6 and R_3 to estimate the settling velocity. He pointed out that the settling shear rate of the laminar-slip regime ranges from 0.1 – 50 sec⁻¹ and the fluid rheological data also should be measured in the same shear-rate range. However, API [12] in its recommended practice suggest use of R_{100}/R_3 for calculating slip velocity of drill cuttings as experienced in an oil well annuli. This study employs all data pairs that could be obtained from the standard Fann 35 VG meter dial readings and corresponding revolutions per minute. Equations 19 and 20 are general equations for determining fluid flow behavior index and consistency index, respectively. The resulted rheological parameters are shown in Tables 1-5. Comparisons are then observed and discussed.

$$n = \frac{\log(\tau_2 / \tau_1)}{\log(\gamma_2 / \gamma_1)} \tag{19}$$

$$K = 0.511 \frac{\tau_2}{\gamma_2^n} \tag{20}$$

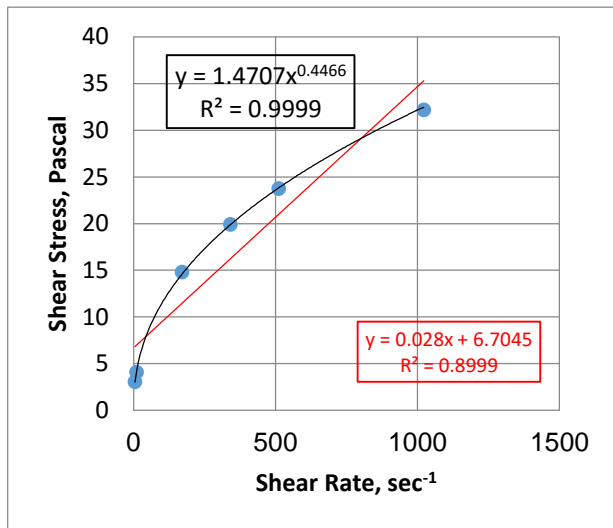


Fig-1: Example drilling fluid rheogram.

4. RESULT AND DISCUSSION

4.1 Predicting Mud Rheogram

Tables 2-7 are a statistical comparison of the accuracy of each specific couple of dial readings and their corresponding shear rates in predicting shear stress for the example fluid. Tables 2-6 contain the values of the example fluid's rheological parameters calculated using different pairs of dial readings and their corresponding shear rates. The shear stress at six Fann 35 VG rpms are calculated again using these rheological parameters.

Table 7 contain the values of the example fluid's rheological parameters calculated from average of the previously calculated values from all different pairs of dial readings as well as rheological parameters estimated from non-linear regression using all available shear stress/shear rate data.

Table-2

Data Pair	R ₆₀₀ /R ₃₀₀	R ₆₀₀ /R ₂₀₀	R ₆₀₀ /R ₁₀₀				
n	0.4381	0.4364	0.4329				
K, Pa.sec ⁿ	1.5464	1.5647	1.6031				
Measured Shear Stress, Pa	Calculated Shear Stress, Pa						
rpm	τ	τ	%E	τ	%E	τ	%E
600	32.19	32.19	0	32.19	0	32.19	0
300	23.76	23.76	0	23.79	0.13	23.85	0.38
200	19.93	19.89	-0.2	19.93	0	20.01	0.4
100	14.82	14.68	-0.94	14.73	-0.61	14.82	0

6	4.09	4.28	4.65	4.31	5.38	4.38	7.09
3	3.07	3.16	2.93	3.19	3.91	3.25	5.86
Average Error, %			1.07		1.47		2.29
Standard Deviation			2.2		2.52		3.27

Table-3

Data Pair	R ₆₀₀ /R ₆	R ₆₀₀ /R ₃	R ₃₀₀ /R ₂₀₀				
n	0.448	0.4435	0.4338				
K, Pa.sec ⁿ	1.4439	1.4896	1.5885				
Measured Shear Stress, Pa	Calculated Shear Stress, Pa						
rpm	τ	τ	%E	τ	%E	τ	%E
600	32.19	32.19	0	32.19	0	32.09	-0.31
300	23.76	23.6	-0.67	23.67	-0.38	23.76	0
200	19.93	19.68	-1.25	19.78	-0.75	19.93	0
100	14.82	14.43	-2.63	14.54	-1.89	14.75	-0.47
6	4.09	4.09	0	4.18	2.2	4.35	6.36
3	3.07	3	-2.28	3.07	0	3.22	4.89
Average Error, %			1.14		0.14		1.75
Standard Deviation			1.13		1.34		3.05

Table-4

Data Pair	R ₃₀₀ /R ₁₀₀	R ₃₀₀ /R ₆	R ₃₀₀ /R ₃				
n	0.4298	0.4499	0.4447				
K, Pa.sec ⁿ	1.6287	1.4368	1.4841				
Measured Shear Stress, Pa	Calculated Dial Reading						
rpm	τ	τ	%E	τ	%E	τ	%E
600	32.19	32.01	-0.56	32.46	0.84	32.34	0.47
300	23.76	23.76	0	23.76	0	23.76	0
200	19.93	19.96	0.15	19.8	-0.65	19.84	0.45
100	14.82	14.82	0	14.49	-2.23	14.58	-1.62
6	4.09	4.42	8.07	4.09	0	4.17	1.96
3	3.07	3.28	6.84	2.99	-2.61	3.07	0
Average Error, %			2.42		0.78		0.21
Standard Deviation			3.93		1.36		1.15

It is clear that using rheological parameters from linear regression show improvement in re-estimating the fluid's rheogram over those values calculated from only two data pairs. Among all other rheological parameters derived from only two data pairs, the parameters obtained from R₆₀₀/R₃ was able to accurately predict the said rheogram with the least average error followed by the parameter obtained from R₃₀₀/R₃. Rheological parameters obtained from R₆/R₃ was the worst to predict the fluid rheogram followed by those obtained using R₂₀₀/R₁₀₀, R₃₀₀/R₁₀₀ and R₆₀₀/R₁₀₀, respectively.

Table-5

Data Pair	R ₂₀₀ /R ₁₀₀	R ₂₀₀ /R ₆	R ₂₀₀ /R ₃				
n	0.4274	0.4518	0.4457				
K, Pa.sec ⁿ	1.6489	1.4303	1.4821				
Measured Shear Stress, Pa	Calculated Shear Stress, Pa						
rpm	τ	τ	%E	τ	%E	τ	%E
600	32.19	31.87	-0.99	32.74	1.71	32.52	1.03
300	23.76	23.7	-0.25	23.94	0.76	23.88	0.51
200	19.93	19.93	0	19.93	0	19.93	0
100	14.82	14.82	0	14.57	-1.69	14.63	-1.28
6	4.09	4.45	8.80	4.09	0	4.18	2.2
3	3.07	3.31	7.82	2.99	-2.61	3.07	0
Average Error, %			2.56		0.31		0.41
Standard Deviation			4.48		1.59		1.17

Table-6

Data Pair	R_{100}/R_6		R_{100}/R_3		R_6/R_3		
n	0.4578		0.4493		0.4150		
K, Pa.sec ⁿ	1.4105		1.4734		1.5582		
Measured Shear Stress, Pa		Calculated Shear Stress, Pa					
rpm	τ	τ	%E	τ	%E	τ	%E
600	32.19	33.66	4.57	33.15	2.98	27.65	-14.1
300	23.76	24.5	3.16	24.28	2.19	20.74	-12.71
200	19.93	20.35	2.11	20.23	1.51	17.53	-12.04
100	14.82	14.82	0	14.82	0	13.15	-11.27
6	4.09	4.09	0	4.19	2.44	4.09	0
3	3.07	2.98	-2.93	3.07	0	3.07	0
Average Error, %		1.15		1.52		8.35	
Standard Deviation		2.68		1.27		6.54	

Table-7

		Ave.	Plot		
n		0.4403	0.4466		
K, Pa.sec ⁿ		1.5193	1.4707		
Measured Shear Stress, Pa		Calculated Shear Stress, Pa			
rpm	τ	τ	%E	τ	%E
600	32.19	32.11	-0.25	32.47	0.87
300	23.76	23.67	-0.38	23.83	0.29
200	19.93	19.8	-0.65	19.88	-0.25
100	14.82	14.59	-1.55	14.59	-1.55
6	4.09	4.23	3.42	4.15	1.47
3	3.07	3.12	1.63	3.05	-0.65
Average Error, %		0.37		0.03	
Standard Deviation		1.82		1.08	

4.2 Settling Velocity

Equations 13 and 15 are used to calculate the settling velocity of the example particle. The result are shown in Figures 2-5. It is obvious that both equations overestimates the particle settling velocity of the example particle (0.7 cm/sec). However equation 13 significantly over estimates the settling velocity (142% average error; SD = 18) more than twice the value observed by Guliyev [18]. While equation 15 shows better predictions as the estimated settling velocity are slightly higher than observed settling velocity (48% average error; SD = 12). This is not strange, as equation 13 do not take into account the irregularity of the particle. According to Wadell [19], if the volume of a particle remains constant, the smaller the value of " ψ ", the larger the fluid drag force on the particle during settling and thus the smaller the settling velocity of the particle. Though the sphericity of the example particle is not significantly less than 1 (0.9), it is however one reason for equation 13 to yield higher predictions. Moreover, the drag coefficient used to derive equation 13 ($C_D = 24/N_{RP} + 1.714$) was lower than that used to derive equation 15 ($C_D = 30/N_{RP} + 67.289/ e^{5.03\psi}$). This is another reason for equation 13 to yield higher predictions.

It is clear that the effect of different rheological parameters that have been used to determine effective viscosity is similar for both equations. In Figure 2, rheological parameters derived from R_{600}/R_{100} (32%

error) followed by R_{600}/R_{200} (39% error) produced the lowest settling velocities compared to R_{600}/R_{300} (42% error), R_{600}/R_3 (53% error) and R_{600}/R_6 (61% error). Though rheological parameters of R_{600}/R_3 predicts well the full rheological spectrum of example fluid, it over estimates the settling velocity.

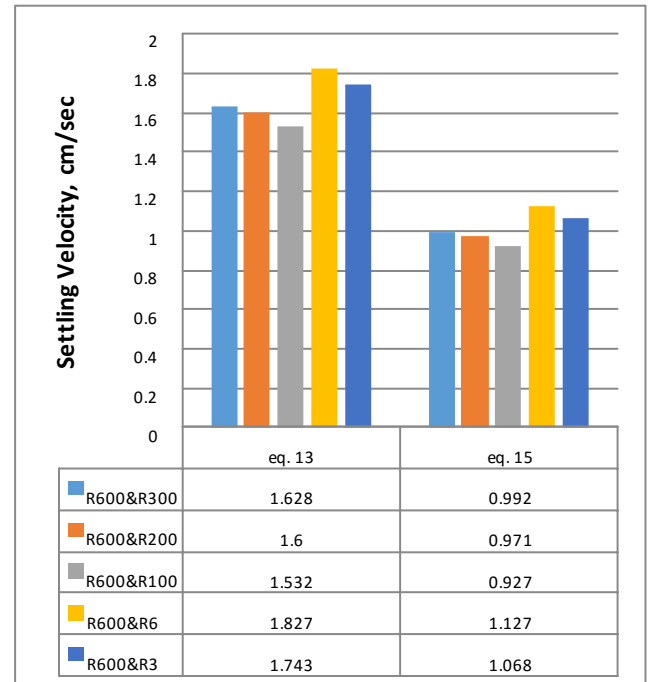


Fig-2: Settling velocities using n & K derived from $R_{600}-R_{300}$, $R_{600}-R_{200}$, $R_{600}-R_{100}$, $R_{600}-R_6$ and $R_{600}-R_3$.

In Figure 3, rheological parameters derived from R_{300}/R_{100} shows the good predictions with approximately 28% error followed by R_{300}/R_{200} (35% error). Rheological parameters derived from R_{300}/R_6 , generated the highest value followed by R_{300}/R_3 (53% error). As has been mentioned earlier, rheological parameters derived from R_{300}/R_3 ranked second in performance for predicting the example fluid rheogram. Similar, to R_{600}/R_3 , rheological parameter of R_{300}/R_3 over predicts the settling velocity compared to other rheological parameters.

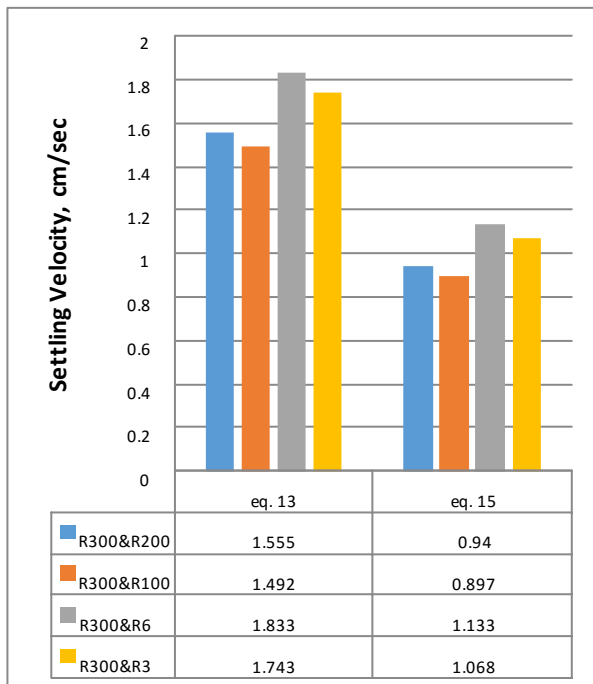


Fig-3: Settling velocities using n & K derived from R₃₀₀-R₂₀₀, R₃₀₀-R₁₀₀, R₃₀₀-R₆ and R₃₀₀-R₃.

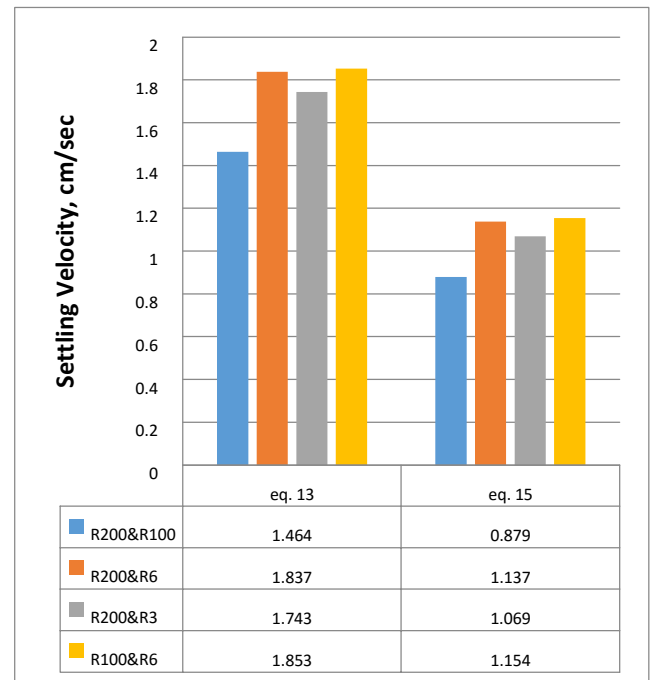


Fig-4: Settling velocities using n & K derived from R₂₀₀-R₁₀₀, R₂₀₀-R₁₀₀, R₂₀₀-R₃ and R₁₀₀-R₆.

The best settling velocity predictions obtained by equation 15 obtained by rheological parameters obtained from R₂₀₀/R₁₀₀ with approximately 26% error. As seen in Figure 4, among all rheological parameters, those derived from R₂₀₀/R₁₀₀ shows the nearest settling velocity value to the observed one (0.879 vs 0.7). Therefore, the best data pairs to predict settling velocity are R₂₀₀/R₁₀₀ followed by R₃₀₀/R₁₀₀ (28% error) and R₃₀₀/R₂₀₀ (35% error).

Figure-5 shows the settling velocities from data pairs as suggested by Chien [8] and API RP 13D [12] together with those derived from average of all rheological parameters derived from all possible data pairs and those obtained by non-linear regression of rheological data. It is clear that approximately all rheological parameters of Figure-5 yielded similar settling velocities. The settling velocities approximately equal to 1 cm/sec which is higher than observed settling velocity (0.7 cm/sec). As seen in Figure-5, the highest percent error was obtained from rheological parameters derived from non-linear regression (55%) followed by those derived from R₁₀₀/R₃ (53%) compared to those of R₆/R₃ (47%) and average (46%). Therefore, it clear that, rheological parameter from data pairs of R₂₀₀/R₁₀₀ followed by R₃₀₀/R₁₀₀ and R₃₀₀/R₂₀₀ out performs those in Figure-5. Generally, all data pairs that do not include R₆ & R₃ have less average % error (34% vs 55%) compared to those that include R₆ & R₃.

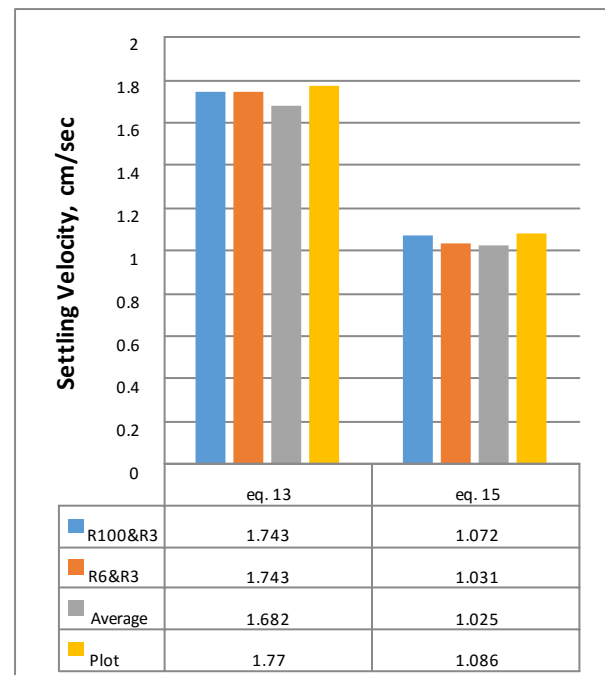


Fig-5: Settling velocities using n & K derived from R₁₀₀-R₃, R₆-R₃, ave., and plot.

To ensure that the obtained results are because of the effect of different rheological parameters not an error of used equations, published equations (equations 14, 16 and 17) have been used to confirm results. Data pairs that showed improved performance to predict settling velocity have been used to calculate settling velocity by different equations (Figure-6). The results have been repeated with

API equation returned slightly good predictions. Again settling velocities from equation 13 and 14 significantly over estimates the settling velocity. The effect of rheological parameters shows similar trends in all equations.

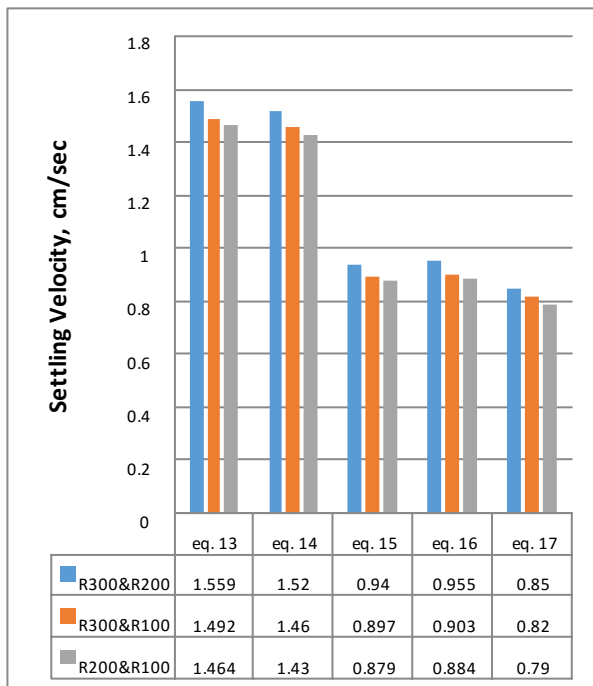


Fig-6: Settling velocities using n & K derived from R₃₀₀-R₂₀₀, R₃₀₀-R₁₀₀, and R₂₀₀-R₁₀₀.

Furthermore, we suggested use of effective velocity at settling shear rate in Moore's correlation instead of his apparent viscosity. Hence, it was possible to make Moore's correlation applicable for stagnant fluids. Data are compared with data pairs that showed best predictions to observed settling velocity, i.e. R₃₀₀/R₂₀₀, R₃₀₀/R₁₀₀, and R₂₀₀/R₁₀₀ (Figure 7). As depicted in Figure-7, modified Moore correlation give overall better predictions at all data pairs of this figure with R₆₀₀/R₃₀₀ and R₂₀₀/R₁₀₀ give the best estimates. Modified Moore correlation was used later to calculate settling velocity using all data pairs (Figures 8 and 9). Generally, all data pairs of Figure-8 give excellent predictions to the observed settling velocity (1.17 average %error; SD=4.62) compared to those of Figure-9 (17.25 average %error; SD = 4.53). Overall, this method obtained approximately 12 average percent error using all data (SD=9) which is significantly less than Chien correlations. The best data pairs to predict the observed settling velocity are R₆₀₀/R₁₀₀ (0.77 %error), R₃₀₀/R₂₀₀ (1.55 %error), R₃₀₀/R₁₀₀ (-2.38 %error), R₆₀₀/R₂₀₀ (4.72 %error), R₂₀₀/R₁₀₀ (-5.2 %error), respectively.

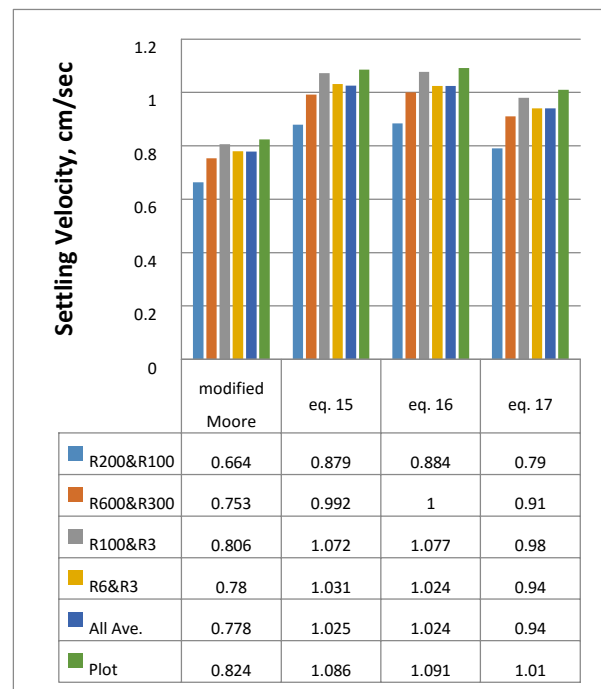


Fig-7: Settling velocities using modified Moore and Chien correlations.

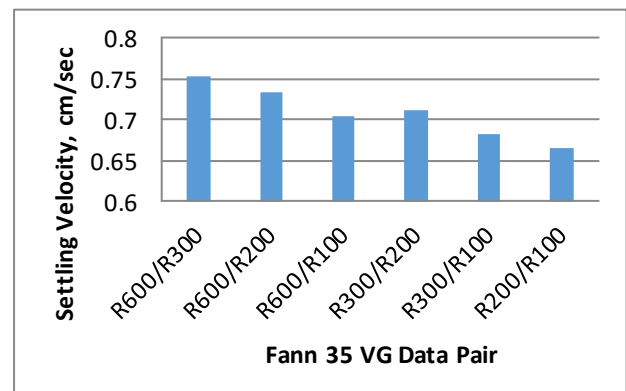


Fig-8: Settling velocities using modified Moore (A).

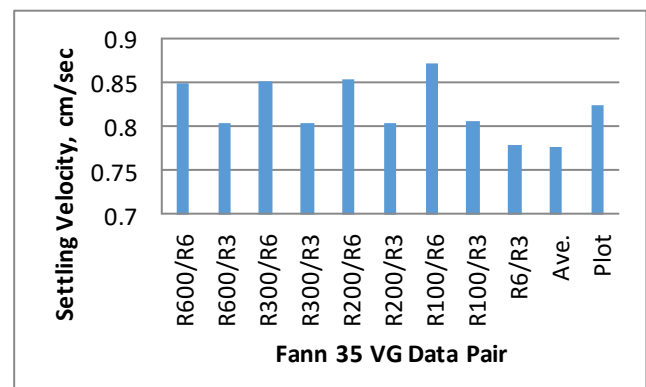


Fig-9: Settling velocities using modified Moore (B). Finally, effects of the rheological parameters and Reynolds number on settling velocity were illustrated. In Figure-10,

flow behavior index was plotted against settling velocities. The variations in magnitude of "n" due to different data pairs from which they are derived spans between 0.42 and 0.46. One single value of "n" departs from this range particularly that derived from R_6/R_3 . The effect was consistent with the settling velocities decreasing when "n" decreased (shear rates $> 1 \text{ sec}^{-1}$: $2.59\text{-}3.39 \text{ sec}^{-1}$). This contradicts with results obtained by other researchers [8]. Chien [8] pointed out that "the effective viscosity will decrease with an increase in i (n) value" particularly for shear rates $> 1 \text{ sec}^{-1}$, therefore, "the settling velocity decreases as the value of i (n) increases".

Therefore it is postulated that lower values of "n" will facilitate hole cleaning at vertical and near vertical sections of the well particularly at laminar flow regimes since the rheological properties of the mud plays a dominant role. However, at higher angles where the drillstring rests against the low side of the well, higher values are always welcomed. Several researchers [20-23] stated that "increasing values of n promote higher fluid velocities under the eccentric drillpipe". Therefore, a compromise must be reached at to balance between these different trends.

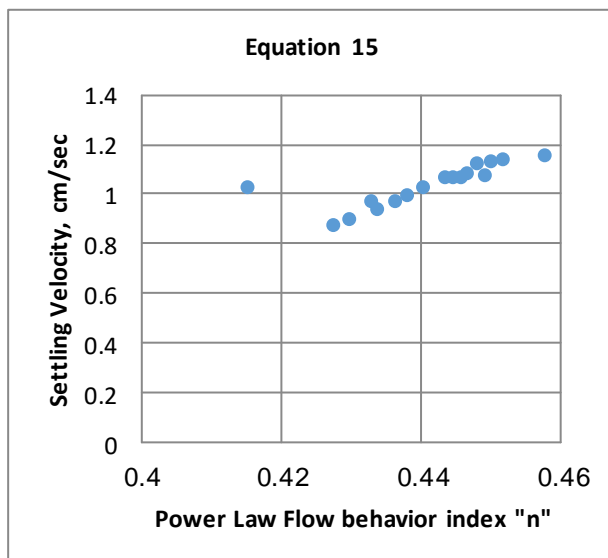


Fig-10: Effect of flow behavior index on settling velocity.

The effect of Reynolds number on settling velocity showed similar trends as "n". As seen in Figure-11, particle Reynolds number varies between 0.02 and 0.04 with different settling velocities and effective viscosities. It is clear that lower values of Reynolds number ensures lower settling velocities. Reynolds number is a ratio between the inertial and viscous forces of liquid. Lower Reynolds number implies a relatively high viscous force of the fluid.

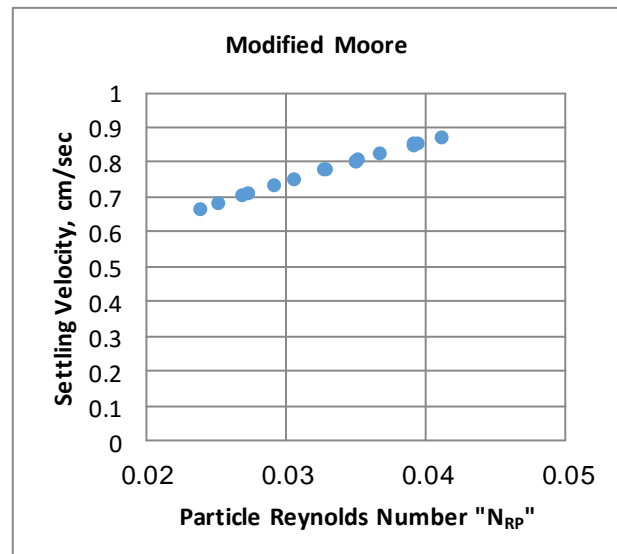


Fig-11: Effect of Reynolds number on settling velocity.

The effect of consistency index, K, on settling velocities has been demonstrated in Figure-12. The effect was completely opposite to the effect of "n". Settling velocities decreased as "K" values increased. This result is in agreement with results of other investigators [8,24]. Chien [8] pointed out that an increase in "K" at a constant value of "n" increases the effective viscosity for a given shear rate and therefore decrease the settling velocity. To elaborate further on this, effective viscosities were plotted against settling velocities and presented in Figure-13. A similar trend as for K values has been obtained.

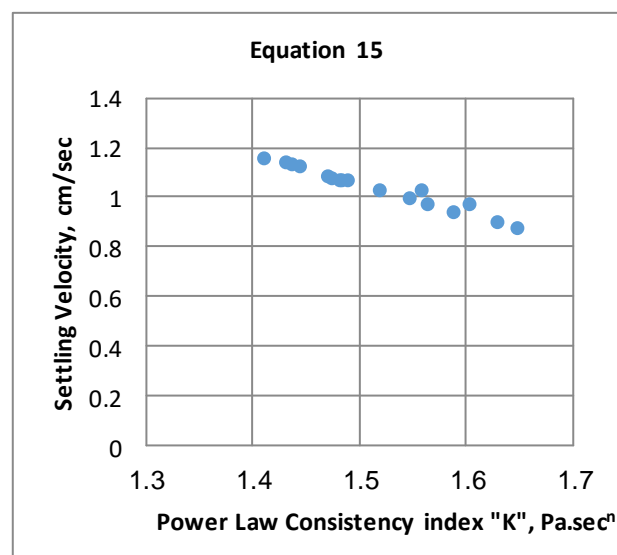


Fig-12: Effect of consistency index on settling velocity.

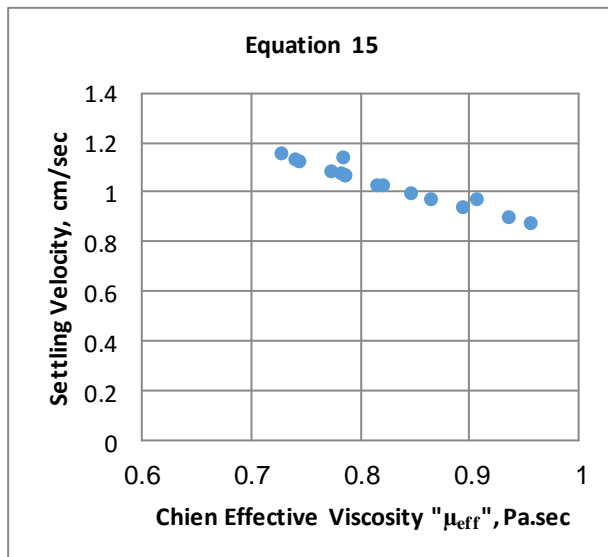


Fig-13: Effect of effective viscosity on settling velocity.

5. CONCLUSIONS

(1) Rheological parameters derived from linear regression was the best to re predict the full rheogram of the fluid. While rheological parameter obtained from R_6/R_3 are the worst to predict the said rheogram.

(2) Among all other rheological parameters derived from only two data pairs, the parameters derived from R_{600}/R_3 was able to accurately describe the fluid rheogram.

(3) Using different data pairs to calculate rheological parameters will definitely affect effective viscosities and settling velocities. The variance in predicted setting velocity values is not negligible.

(4) For Chien correlations, good settling velocity predictions were obtained using rheological parameter obtained from R_{200}/R_{100} followed by R_{300}/R_{100} and R_{300}/R_{200} .

(5) For Chien correlations, commonly used data pairs (R_{600}/R_{300}) as well as data pairs suggested by Chien [8] and API [12] recommended practice resulted in rheological parameters that over predicts settling velocities compared to their counter parts, i.e. R_{200}/R_{100} , R_{300}/R_{100} .

(6) Settling velocities obtained from modified Moore correlation were nearly identical to observed velocity particularly with R_{600}/R_{200} , R_{600}/R_{100} , R_{300}/R_{200} , R_{300}/R_{100} and R_{200}/R_{100} .

(7) Settling velocity where found to decrease with decreased "n" values, something which is not welcomed at highly deviated and horizontal wellbore. Lower value impede flow diversion below the eccentric drillpipe.

(8) Higher values of K promotes higher effective viscosities and results in lower settling velocities. This trend is opposite to that of "n".

NOMENCLATURE

A_p = Projected area of Particle, cm^2

A_S	= Projected area of a sphere of same vol., cm^2
C_D	= Drag Coefficient, dimensionless
D_p	= Particle diameter, cm
d_H	= Hole inside diameter, cm
d_p	= Drillpipe outside diameter, cm
F_D	= Drag force on particle, dyne
F_g	= Gravitational force on particle, dyne
F_B	= Buoyancy force on particle, dyne
F_{eff}	= Effective force on particle, dyne
g	= Acceleration due to gravity, 981 cm/sec^2
K	= Power law consistency index, $\text{Pa}\cdot\text{sec}^n$
n	= Power law flow behaviour index, dimensionless
N_{RP}	= Particle Reynolds number, dimensionless
R_3	= Fann dial reading at 3 rpm
R_6	= Fann dial reading at 6 rpm
R_{100}	= Fann dial reading at 100 rpm
R_{200}	= Fann dial reading at 200 rpm
R_{300}	= Fann dial reading at 300 rpm
R_{600}	= Fann dial reading at 600 rpm
U_p	= Particle terminal velocity, cm/sec
U_a	= Fluid annular velocity, cm/sec
V	= Particle volume, cm^3

Greek Symbols

γ	= Shear rate, sec^{-1}
γ_1	= Lower shear rate, sec^{-1}
γ_2	= Higher shear rate, sec^{-1}
τ	= Shear stress, Pa
τ_1	= Lower Shear stress, Pa
τ_2	= Higher Shear stress, Pa
π	= Constant = 3.14
ρ_l	= Liquid density, g/cm^3
ρ_p	= Particle density, g/cm^3
μ_a	= Moore's apparent viscosity, $\text{mPa}\cdot\text{sec} = \text{cP}$
μ_e	= Chien's effective viscosity, $\text{mPa}\cdot\text{sec} = \text{cP}$
ψ	= Particle sphericity, dimensionless ($\psi = A_S / A_P$)

REFERENCES

- [1] S. Tian and G. H. Medly, "Re-Evaluating Hole Cleaning in Underbalanced Drilling Applications," IADC Underbalanced Drilling Conference and Exhibition, Aug. 28-29, Houston, Texas, 2000.
- [2] M. N. Belavadi and G. A. Chukwu, "Experimental Study of the Parameters Affecting Cutting Transportation in a Vertical Wellbore Annulus," SPE Western Regional Meeting, Mar. 23 - 25, Long Beach, California, SPE 27880, 1994.
- [3] S. F. Chien "Annular Velocity for Rotary Drilling Operations," *Intl. J. Rock Mech. Min. Sci.*, vol. (9), pp. 403, 1972.
- [4] H. U. Zeidler, "An Experimental Analysis of the Transport of Drilling Particles," *SPEJ*, vol. 14 (1), pp. 39-48, SPE 3064, 1972.

- [5] P. L. Moore, "Drilling Practice Manual," PennWell Publishing Co., Tulsa, pp. 268-276, 1974.
- [6] R. E. Walker and T. M. Mayes "Design of Muds for Carrying Capacity," *JPT*, vol. 27 (7), July, pp. 893, SPE 4975, 1975.
- [7] J. M. Peden and Y. Luo, "Settling Velocity of Various Shaped Particles in Drilling and Fracturing Fluids," *SPEDE*, vol. 2 (4), Dec, pp. 337-343, SPE 16243, 1987.
- [8] S. F. Chien, "Settling Velocity of Irregularly Shaped Particles," *SPEDC*, vol. 9 (4), Dec, pp. 281-289, SPE 26121, 1994.
- [9] K. J. Sample, and A. T. Bourgoyne, "An Experimental Evaluation of Correlations Used for Predicting Cutting Slip Velocity," SPE Annual Technical Conference and Exhibition, Oct. 9-12, Denver, Colorado, SPE 6645, 1977.
- [10] P. Skalle, K. R. Backe, S. K. Lyomov, and J. Sveen, "Barite Segregation in Inclined Boreholes," *Journal of Canadian Petroleum Technology*, special vol., PETSOC 97-76, 1999.
- [11] T. Hemphill, "Hole-Cleaning Model Evaluated Fluid Performance in Extended Reach Wells," *Oil & Gas Journal*, Jul. 14, pp. 56-64, 1997.
- [12] American Petroleum Institute, "Recommended Practice on the Rheology and Hydraulics of Oil-Well Drilling Fluids," API Recommended Practice 13D, Third Edition, pp. 20-21, June, 1995.
- [13] M. S. Bizanti and S. Robinson, "PC Program Speeds Slip-Velocity Calculations," *Oil & Gas Journal*, Nov. 7, pp. 44-45, 1988.
- [14] T. E. Becker, J. J. Azar and S. S. Okrajni, "Correlations of Mud Rheological Properties with Cuttings-Transport Performance in Directional Drilling," *SPEDE*, vol. 6 (1), Mar, pp. 16-24, SPE 19535, 1991.
- [15] Y. Luo, "Cuttings Transport through Drilling Annuli at Various Angles," PhD dissertation, Heriot-Watt Uni., 1988.
- [16] M. Zamora and F. Growcock, "The Top 10 Myths, Misconceptions and Mysteries in Rheology and Hydraulics," AADE Fluid Conference and Exhibition, Apr. 6-7, Houston, Texas, AADE-10-DF-HO-40, 2010.
- [17] T. Hemphill, W. Campos and A. Pilehavari, "Yield-Power Law Model Accurately Predicts Mud Rheology," *Oil & Gas Journal*, Aug. 23, pp. 91-49.
- [18] E. Guliyev, "The Importance of Low-end-rheology and its Influence on Particle Slip Velocity," Master thesis, Norwegian University of Science and Technology, 2013.
- [19] H. Waddell, "The Coefficient of Resistance as a Function of Reynolds Number for Solids of Various Shape," *J. Franklin Inst.*, pp. 459, 1934.
- [20] T. Hemphill and T. Larsen, "Hole Cleaning Capabilities of Water-Based and Oil-Based Drilling Fluids: A comparative, Experimental Study," Annual Technical Conference and Exhibition, Houston, Texas, Oct. 3-6, SPE 26328, 1989.
- [21] P. Kenny and T. Hemphill, "Hole-Cleaning Capabilities of an Ester-Based Drilling Fluid System," *SPEDE*, vol. 11 (1), March, SPE 28308, 1996.
- [22] P. Kenny, E. Sunde and T. Hemphill, "Hole Cleaning Modelling: What's "n" Got To Do With it?," IADC/SPE Drilling Conference, Mar. 12-15, New Orleans, Louisiana, IADC/SPE 35099, 1996.
- [23] M. Hacıislamoglu, "Non-Newtonian Flow in Eccentric Annuli and Its Application to Petroleum Engineering Problems," PhD dissertation, Louisiana State U., Baton Rouge, 1989.
- [24] R. A. Eltilib, H. H. Al Kayiem and A. Jaafar, "Investigation on the Particle Settling Velocity in Non-Newtonian Fluids," *Journal of Applied Science*, vol. 11 (9), pp. 1528-1535, 2011.

BIOGRAPHIES



Mazen A. Muherei is an assistant professor in Petroleum Eng. Dept. at Hadhramout Uni., Yemen. He obtained his BSc in Petroleum Eng. from Faculty of Petroleum and Mining Eng., Suez Canal Uni. in 1997. He get his MSc and PhD degrees in Petroleum Eng. in 2003 and 2009 respectively, from Universiti Teknologi Malaysia, Johor Bahru, Malaysia.



Saeed S. Basaleh is an assistant professor in Petroleum Eng. Dept. at Hadhramout Universit, Yemen. He holds MSc in oil well excavation Eng. Technology and a PhD in Technology and Eng. of Geological explorations, both from Russian State Geological Prospecting University n. a. Sergo Ordzhonikidze.